heterogeneity of the DLBCL component using morphological, immunohistochemical, and FISH analyses.

FL transformed most commonly to the DLBCL centroblastic subtype,[4] but occasionally to the DLBCL anaplastic subtype with CD30 expression.[5] We confirmed that most of the DLBCLs were of the centroblastic subtype, with two exceptional cases of the anaplastic subtype.

CD10 shows restricted expression in germinal center B-cells of reactive lymphoid tissue. Although the reported frequency of CD10 expression in FL varies, about 60% of FLs express CD10.[4] However, no previous report has documented changes in CD10 expression through transformation from low-grade FL to DLBCL. In this study, 14 DLBCLs were negative for CD10, and among them, six showed loss of CD10 expression through transformation. Previous reports have indicated that CD10 expression is often stronger in follicles than in interfollicular neoplastic cells, and that the frequency of CD10 expression is lower in FL grade 3 than in low-grade FL.[24] It is suggested that loss of CD10 expression through FL transformation is possible in the process of escape from the follicular dendritic cell meshwork and diffusion, and tumor cell enlargement.

Bcl-2 is expressed on resting and B and T cells, but not on normal germinal center cells. Bcl-2 protein has an antiapoptotic function,[25] and is expressed in the majority of FLs ranging from nearly 100% in grade 1–75% in grade 3,[26] and in about 30–50% of de novo DLBCLs.[23] Bcl-6 is expressed in germinal center B-cells and a subset of $CD4^+$ T cells.[27] Bcl-6 is expressed in 88% of FLs,[28] and 55–97% of de novo DLBCLs.[29] Most of the DLBCLs that had transformed from FL retained a high frequency of Bcl-2 and Bcl-6 expression, which tended to be higher than that in de novo DLBCL. Because Bcl-2 and Bcl-6 expression was retained during transformation in most cases, Bcl-2 and Bcl-6 positivity might be a precondition for transformation of DLBCL from FL.

MUM1 is a lymphoid-specific member of the interferon regulatory factor family of transcription factors.[30] MUM1 is normally expressed in plasma cells and a minor subset of germinal center B cells, and has been reported to be expressed in 50–77% of DLBCLs.[31–33] In this study, MUM1 was positive in 16% of low-grade FLs and 34% of DLBCLs. This rate was lower than that in de novo DLBCL, but it was surprising that 34% of transformed FLs expressed MUM1. Twenty cases that were MUM1-positive in both the FL and DLBCL components were suggested to be derived from germinal center MUM1-positive B cells, and seven cases showing MUM1-gain indicated that this event was not infrequent during FL transformation.

CD30 was positive in Hodgkin and Reed-Sternberg cells of classical Hodgkin lymphoma, anaplastic large cell lymphoma, anaplastic variant of DLBCL, and a subset of non-neoplastic activated B and T cells.[1,5] Most FLs contain a small number of CD30-positive cells, located mainly at the edge of the neoplastic follicles,[34] and we confirmed this feature. Transformation of FL into CD30-positive large B-cell lymphoma with anaplastic features has been reported.[5] In this study, 20% of the cases gained CD30 expression in DLBCL, which included two cases of the DLBCL anaplastic variant, indicating that CD30-positive large lymphoid cells tended to increase gradually during transformation.

CD5 is reported to be an unfavorable prognostic marker in de novo DLBCL.[35] Richiter's syndrome, a transformant of chronic lymphocytic leukemia/small lymphocytic lymphoma, is a well-known secondary $CD5^+$ DLBCL. Manazza *et al.* reported that CD5 and CD10-double-positive FL transformed to $CD5^+$ DLBCL.[36] Our present study is the first to indicate that $CD5^-$/$CD10^+$ FL with IGH/BCL2 fusion can transform to secondary $CD5^+$/$CD10^-$ DLBCL with IGH/BCL2 fusion.

Notably, our series included one case of classical Hodgkin lymphoma that had transformed from FL via DLBCL. Previous reports have suggested that composite follicular lymphoma and Hodgkin lymphoma represent two morphologic manifestations of the same tumor clones.[8,9] In the present case, IGH/BCL2 fusion was detected in both the FL and the Hodgkin/Reed-Sternberg cells by FISH analysis, strongly suggesting transformation from FL.

Although transformed FL is generally considered to have a GCB phenotype, we demonstrated that a proportion of FLs can show a dramatic change in immunophenotype through transformation. Davies *et al.*[18] examined 35 cases of transformed FL, and found that 89% of them had a GCB phenotype and 9% had a non-GCB phenotype. In our study, six (16%) of the DLBCLs had a non-GCB phenotype. Some previous studies examining the difference in prognosis between patients with a GCB phenotype *versus* those with non-GCB-phenotype DLBCL revealed that the former group had a more favorable prognosis.[15,16] However, Colomo *et al.* found no prognostic difference between them,[37] and recently therefore this issue has been controversial. In the present study, GCB *versus* non-GCB was not a significant prognostic factor. However, as the number of cases was small, further studies are necessary to clarify the prognostic difference between GCB and non-GCB in transformed FL.

We detected a high relative frequency (82%) of IGH/BCL2 fusion in transformed FL. Although the rate is higher than that in Japanese FL, it is almost equal to that in FL grade 1 (10/12, 83%).[21] Because the present cases of DLBCL had transformed from low-grade FL, we were unable to conclude whether cases showing IGH/BCL2 fusion transformed more frequently than cases without it.

In conclusion, our study has clearly demonstrated heterogeneity of the immunophenotype in DLBCL transformed from low-grade FL, suggesting that various mechanisms may affect FL transformation. As many genetic changes including c-MYC amplification and p53 mutation have been detected in transformed FL, it will be necessary to analyze the relationship between these genetic abnormalities and morphological, immunohistochemical, and IGH/BCL2 fusion status in transformed FL.

Acknowledgments

The authors would like to thank C. Kina and S. Miura for technical assistance with immunohistochemistry. This work was supported in part by a Grant-in-Aid for Cancer Research from the Ministry of Health, Labor, and Welfare of Japan.

References

1 A clinical evaluation of the International Lymphoma Study Group Classification of Non-Hodgkin's Lymphoma. The non-Hodgkin's Lymphoma Classification Project. *Blood* 1997; **89**: 3909–18.
2 Horning SJ, Rosenberg SA. The natural history of initially untreated low-grade non-Hodgkin's lymphoma. *N Eng J Med* 1984; **311**: 1471–5.
3 Gallagher CJ, Gregory WM, Jones AE *et al.* Follicular lymphoma: prognostic factors for response and survival. *J Clin Oncol* 1986; **4**: 1470–80.
4 Harris NL, Ferry JA. Follicular lymphoma. In: Knowles DM, ed. *Neoplastic Hematopathology*, 2nd edn. Philadelphia, PA: Lippincott Williams & Wilkins, 2001; 823–53.
5 Alsabeh R, Medeiros LJ, Glackin C *et al.* Transformation of follicular lymphoma into CD30-large cell lymphoma with anaplastic cytologic features. *Am J Surg Pathol* 1997; **21**: 528–36.
6 Yano T, Jaffe ES, Longo DJ *et al.* MYC rearrangements in histologically progressed follicular lymphomas. *Blood* 1992; **80**: 758–67.
7 de Jong D, Voetdujk B, Bavestock G *et al.* Activation of the c-myc oncogene in a precursor B-cell blast crisis of follicular lymphoma, presenting as composite lymphoma. *N Eng J Med* 1998; **318**: 1373.
8 Brauninger A, Hansmann ML, Strickler JG *et al.* Identification of common germinal-center B-cell precursors in two patients with both Hodgkin's disease and non-Hodgkin's lymphoma. *N Eng J Med* 1999; **340**: 1239–47.
9 Marafioti T, Hummel M, Anagnostopoulos I *et al.* Classical Hodgkin's disease and follicular lymphoma originating from the same germinal center B cell. *J Clin Oncol* 1999; **17**: 3804–9.

10 Sander CA, Yano T, Clark HM *et al.* p53 mutation is associated with progression in follicular lymphomas. *Blood* 1993; **82**: 1994–2004.
11 Lo Coco F, Gaidano G, Louie DC *et al.* p53 mutations are associated with histologic transformation of follicular lymphoma. *Blood* 1993; **82**: 2289–95.
12 Pinyol M, Cobo F, Bea S *et al.* p16 (INF4a) gene inactivation by deletions, mutations, and hypermethylation is associated with transformed and aggressive variants of non-Hodgkin's lymphomas. *Blood* 1998; **91**: 2977–84.
13 Elenitoba-Johnson KS, Gascoyne RD, Lim MS *et al.* Homozygous deletions at chromosome 9p21 involving p16 and p15 are associated with histologic progression in follicle center lymphoma. *Blood* 1998; **91**: 4677–85.
14 Tilly H, Rossi A, Stamatoullas A *et al.* Prognostic value of chromosomal abnormalities in follicular lymphoma. *Blood* 1994; **84**: 1043–9.
15 Alizadeh AA, Eisen MB, Davis RE *et al.* Distinct types of diffuse large B-cell lymphoma identified by gene expression profiling. *Nature* 2000; **403**: 503–11.
16 Rosenwald A, Wright G, Chan WC *et al.* The use of molecular profiling to predict survival after chemotherapy for diffuse large B-cell lymphoma. *N Eng J Med* 2002; **346**: 1937–47.
17 Hans SP, Weisenburger DD, Greiner TC *et al.* Conformation of molecular classification of diffuse large B-cell lymphoma by immunohistochemistry using a tissue microarray. *Blood* 2004; **103**: 275–82.
18 Davies AJ, Rosenwald A, Wright G *et al.* Transformation of follicular lymphoma to diffuse large B-cell lymphoma proceeds by distinct oncogenic mechanisms. *Br J Haematol* 2007; **136**: 286–93.
19 Godon A, Moreau A, Talmant P *et al.* Is t(14;18) (q32;q21) a constant finding in follicular lymphoma? An interphase FISH study on 63 patients. *Leukemia* 2003; **17**: 255–9.
20 Biagi JJ, Suymour JF. Insights into the molecular pathogenesis of follicular lymphoma arising from analysis of geographic variation. *Blood* 2002; **99**: 4265–75.
21 Sekiguchi N, Kobayashi Y, Yokota Y *et al.* Follicular lymphoma subgrouping by fluorescence in situ hybridization analysis. *Cancer Sci* 2005; **96**: 77–82.
22 Leoncini L, Delsol G, Gascoyne RD *et al.* Aggressive B-cell lymphomas: a review based on the workshop of the XI meeting of the European association for haematopathology. *Histopathology* 2005; **46**: 241–55.
23 Jaffe ES, Harris NL, Stein H *et al. World Health Organization Classification of Tumors, Pathology and Genetics, Tumours of Haematopoietic and Lymphoid Tissues*. Lyon: IARC Press, 2001; **162–167**: 171–4.
24 Dogan AMQ, Aiello A *et al.* Follicular lymphomas contain a clonally linked but phenotypically distinct neoplastic B-cell population in the interfollicular zone. *Blood* 1998; **91**: 4708–14.
25 Nunez G, London L, Hockenbery D *et al.* Deregulated Bcl-2 gene expression selectively prolongs survival of growth factor-deprived hemoopietic cell lines. *J Immunol* 1990; **144**: 3602–10.
26 Lai R, Arber DA, Chang KL *et al.* Frequency of bcl-2 expression in non-Hodtkin lymphoma: a study of 778 cases with comparison of marginal zone lymphoma and monocytoid B-cell hyperplasia. *Mod Pathol* 1998; **11**: 864–9.
27 Falini B, Fizzotti M, Pileri S *et al.* Bcl-6 protein expression in normal and neoplastic lymphoid tissues. *Ann Oncol* 1997; **8**: 101–4.
28 Peh SC, Shaminie J, Tai YC *et al.* The pattern and frequency of t(14;18) translocation and immunophenotype in Asian follicular lymphoma. *Histopathology* 2004; **45**: 501–10.
29 Anagnostopoulos I, Dallenbach F, Stein H. Diffuse large cell lymphomas. In: Knowles DM, ed. *Neoplastic Hematopathology*, 2nd edn. Philadelphia, PA: Lippincott Williams & Wilkins, 2001; 860.
30 Mamane Y, Heylbroeck C, Genin P *et al.* Interferon regulatory factors: the next generation. *Gene* 1999; **237**: 1–14.
31 Natkunam Y, Warnke RA, Montgomery K *et al.* Analysis of MUM1/IRF4 protein expression using tissue microarrays and immunohistochemistry. *Mod Pathol* 2001; **14**: 686–94.
32 Falini B, Fizzotti M, Pucciarini A *et al.* A monoclonal antibody (MUM1p) detects expression of the MUM1/IRF4 protein in a subset of germinal center B cells, plasma cells, and activated T cells. *Blood* 2000; **95**: 2084–92.
33 Tsuboi K, Iida S, Inagaki H *et al.* MUM1/IRF4 expression as a frequent event in mature lymphoid malignancies. *Leukemia* 2000; **14**: 449–56.
34 Piris M, Gatter KC, Mason DY. CD30 expression in follicular lymphoma. *Histopathology* 1991; **18**: 25–9.
35 Yamaguchi M, Seto M, Okamoto M *et al.* De novo CD5$^+$ diffuse large B-cell lymphoma: a clinicopathologic study of 109 patients. *Blood* 2002; **99**: 815–21.
36 Manazza AD, Bonello L, Pagano M *et al.* Follicular origin of a subset of CD5$^+$ diffuse large B-cell lymphomas. *Am J Clin Pathol* 2005; **124**: 182–90.
37 Colomo L, Lopez-Guillermo A, Perales M *et al.* Clinical impact of the differentiation profile assessed by immunophenotyping in patients with diffuse large B-cell lymphoma. *Blood* 2003; **101**: 78–84.

doi: 10.1111/j.1349-7006.2008.00873.x

Histological and immunophenotypic changes in 59 cases of B-cell non-Hodgkin's lymphoma after rituximab therapy

Akiko Miyagi Maeshima,[1,4] Hirokazu Taniguchi,[1] Junko Nomoto,[2] Dai Maruyama,[2] Sung-Won Kim,[2] Takashi Watanabe,[2] Yukio Kobayashi,[2] Kensei Tobinai[2] and Yoshihiro Matsuno[3]

[1]Clinical Laboratory; [2]Hematology and Stem Cell Transplantation Divisions, National Cancer Center Hospital, Tokyo; [3]Department of Surgical Pathology, Hokkaido University Hospital, Sapporo, Japan

(Received June 30, 2008/Revised September 4, 2008/Accepted September 12, 2008/Online publication November 25, 2008)

Rituximab is a chimeric monoclonal antibody that recognizes the CD20 antigen. It has been used to treat B-cell non-Hodgkin lymphoma (B-NHL), but recently rituximab resistance has been a cause for concern. We examined histological and immunohistochemical changes in 59 patients with B-NHL after rituximab therapy. The patients comprised 32 men and 27 women with a median age of 59 years. Pre-rituximab specimens comprised 34 follicular lymphomas (FL), 11 diffuse large B-cell lymphomas (DLBCL), 10 mantle cell lymphomas, two marginal zone B-cell lymphomas (MZBCL), and two chronic lymphocytic leukemias (CLL). CD20 expression in lymphoma cells was evaluated by immunohistochemistry or flow cytometry. Post-rituximab materials were taken a median of 6 months (4 days to 59 months) after rituximab therapy. Sixteen cases (27%) showed loss of CD20 expression with four histological patterns: pattern 1, no remarkable histological change (FL, 5; DLBCL, 3; and CLL, 2); pattern 2, proliferation of plasmacytoid cells (FL, 2; DLBCL, 1; and MZBCL, 1); pattern 3, transformation to classical Hodgkin's lymphoma (FL, 1); and pattern 4, transformation to anaplastic large cell lymphoma-like undifferentiated lymphoma (FL, 1). Loss of CD20 was unrelated to the interval of biopsies, treatment regimen, clinical response, and frequency of rituximab administration. Loss of CD20 within 1 month of rituximab therapy (3/14, 21%) and regain of CD20 (2/7, 29%) were not frequent. CD20-positive relapse with transformation occurred most frequently in cases of early relapse. In conclusion, B-NHL showed various histological and immunophenotypic changes after rituximab therapy, including not only CD20 loss but also proliferation of plasmacytoid cells or transformation to special subtypes of lymphoma. (*Cancer Sci* 2009; 100: 54–61)

Rituximab is a chimeric monoclonal antibody that has recently been incorporated into the treatment of B-cell non-Hodgkin lymphoma (B-NHL). It recognizes the CD20 antigen, a pan-B-cell marker, binds to it, and induces apoptosis of CD20-positive cells.[1–4] Rituximab can be used as a monotherapy or in combination with conventional chemotherapy for treatment of low- and high-grade, untreated, relapsed, or refractory CD20-positive B-NHL, achieving a high response rate with a low toxicity.

Recent studies have reported that B-NHL show CD20-negative relapse after rituximab therapy.[5–17] Transformation of follicular lymphoma (FL) to CD20-negative diffuse large B-cell lymphoma (DLBCL),[15] proliferation of CD20-negative plasmacytoid tumor cells of marginal zone B-cell lymphoma (MZBCL)[16] or lymphoplasmacytic lymphoma,[13] transformation of FL to classical Hodgkin's lymphoma,[17] and progression of nodular lymphocyte-predominant Hodgkin lymphoma to CD20-negative T-cell-rich B-cell lymphoma have also been reported.[18]

Several mechanisms of resistance to rituximab have been suggested, including selection of a CD20-negative clone as a consequence of rituximab exposure, masking of CD20 epitopes by rituximab itself, or true loss of CD20 antigen by genetic and epigenetic changes.[12,13,15,19–24]

In the present study we carried out retrospective analyses of histological and immunophenotypic changes and outcome in 59 patients with B-NHL after rituximab-containing therapy, to explore the effect of rituximab on CD20 expression and morphology in B-NHL.

Materials and Methods

Patient selection. We reviewed the pathology archives of the National Cancer Center Hospital, Tokyo, Japan, for the period 2002 to 2007. Fifty-nine consecutive cases of CD20-positive B-NHL treated with rituximab, with or without chemotherapy, for which pre- and post-rituximab specimens were available, were included in our study. Rituximab (Zenyaku Kogyo, Tokyo, Japan) was used at a standard dose of 375 mg/m^2 once a week for rituximab monotherapy and once every 3 weeks for the rituximab-cyclophosphamide, doxorubicin, vincristine and prednisone (CHOP) regimen. Clinical information was extracted from the medical records, and the Ann Arbor system was used for staging.

Histological review. Biopsy or surgical specimens were fixed in 10% neutral-buffered formalin overnight, embedded in paraffin, cut into sections 4 μm thick, and stained with hematoxylin–eosin for histological evaluation. All of the pre-rituximab specimens were CD20-positive B-NHL by definition, and post-rituximab specimens included any lymphomas. All of the specimens were reviewed by three pathologists (A.M.M., H.T., and Y.M.) to confirm that the morphological characteristics fulfilled the criteria of the World Health Organization classification of lymphoid neoplasms, 2001.[25] Histological subtype, loss of CD20 expression by immunohistochemistry or flow cytometry, presence or absence of plasmacytoid differentiation, and the relationship between histological transformation and CD20 loss were examined.

Immunohistochemistry, flow cytometry, *in situ* hybridization, and interphase fluorescence *in situ* hybridization analyses. We carried out immunohistochemical staining on formalin-fixed paraffin-embedded pre- and post-rituximab specimens using a panel of monoclonal and polyclonal antibodies. Sections 4 μm thick were cut from each paraffin block, deparaffinized, and incubated

[4]To whom correspondence should be addressed. E-mail: akmaeshi@ncc.go.jp

doi: 10.1111/j.1349-7006.2008.01005.x

at 121°C in pH 6.0 citrate buffer for 10 min for antigen retrieval. Antibodies included those against the following antigens: CD3 (clone PS1, ×25; Novocastra, Newcastle, UK; polymer method), CD20 (L26, ×100; Dako, Glostrup, Denmark; labeled streptavidin–biotin method [LSAB]), and CD79a (JCB117, ×100; Dako; LSAB) routinely; and CD5 (4C7, ×50, Novocastra; polymer), CD7 (CD7-272, ×100; Novocastra; avidin–biotin complex method [ABC]), CD10 (56C6, ×50; Novocastra; polymer), CD15 (MMA, ×100; Becton Dickinson, Franklin Lakes, NJ, USA; polymer), CD30 (Ber-H2, ×100; Dako; polymer), CD45 (2B11 + PD7/26, ×100; Dako; LSAB), CD45RO (UCHL1, ×50; Dako; LSAB), CD56 (1B6, ×100; Novocastra; LSAB), ALK (ALK1, ×200; Dako; polymer), Bcl-2 (124, ×100; Dako; LSAB), Bcl-6 (poly, ×50; Dako; ABC), cyclin D1 (SP4, ×25; Nichirei, Tokyo, Japan; polymer), TIA-1 (26gA10F5, ×1000; Immunotech, Marseille, France; polymer), granzyme B (GrB-7, ×200; Dako; polymer), MPO (poly, ×1000; Dako; LSAB), MUM1 (MUM1p, ×50; Dako; ABC), PAX5 (24, ×200; Becton Dickinson; ABC), TdT (poly, ×100; Dako; polymer), Igκ (poly, ×20 000; Dako; LSAB), Igλ (poly, ×40 000; Dako; LSAB), IgA (poly, ×100 000; Dako; polymer), IgG (poly, ×20 000; Dako; polymer), and IgM (poly, ×20 000; Dako; polymer) optionally. The percentages of CD20-positive tumor cells were counted semiquantitatively by immunohistochemistry (IHC). Immunoreactivity for CD20 was judged positive (no CD20 loss) if >95% of the tumor cells were stained, partially negative (partial CD20 loss) if 10–95% of the cells were stained, or negative (CD20 loss) if <10% of the cells were stained. When a post-rituximab specimen showed loss of CD20 expression, it was judged as B-cell lineage if there was positivity for CD79a.

Flow cytometry was carried out using an Epics XL-MCL instrument with System II Software (Beckman Coulter). The flow cytometry panel included CD20 (B-Ly1), CD19 (HD37), Igκ (poly), and Igλ (poly) (Dako). Fluorescence *in situ* hybridization (FISH) and *in situ* hybridization (ISH) analyses were optional. Sections 4 μm thick were cut from each paraffin block and used for FISH analysis. Judgment of the fusion gene was carried out as described previously.[26] Dual-color LSI IGH Spectrum Green/LSI BCL2 Spectrum Orange Dual Fusion Translocation Probes (Vysis, Downers Grove, IL, USA) were used to detect t(14;18): IGHBCL2 fusion. ISH with Epstein–Barr-encoded RNA (EBER-1) probes (Dako) was carried out in some cases to detect possible Epstein–Barr virus infection.

Statistical analysis. The relationships between CD20 expression and treatment regimen (rituximab monotherapy vs combination therapy with rituximab and chemotherapy), response (complete response [CR] vs others, or overall response [OR] vs others), frequency of rituximab administration, and interval between the last dose of rituximab and rebiopsy were examined by χ^2-test or Mann-Whitney *U*-test. Differences were considered significant when the *P*-value was less than 0.05.

Results

Patient characteristics. Clinical information for all consecutive 59 patients is summarized in Table 1. The patients comprised 32 men and 27 women, ranging in age from 37 to 80 years with a median age of 59 years. Eight patients had stage I/II disease and 51 patients had stage III/IV disease. All of the patients received rituximab by definition, with or without chemotherapy (CHOP or other types of regimen). The 59 patients received a median of six courses (range 1–17) of rituximab. The median interval between the last dose of rituximab and rebiopsy was 6 months (range 4 days to 59 months). The overall response rate was 79% and the % CR was 46% to rituximab-containing regimens.

Four histological patterns of CD20 loss. The results of histological analysis and immunohistochemical staining for each antibody are summarized in Tables 1–2. The total of 59 pre-rituximab B-NHL specimens included 34 FL with or without a DLBCL component, 11 DLBCL, 10 mantle cell lymphomas (MCL), two MZBCL, and two chronic lymphocytic leukemias (CLL). We considered that the following two factors may have contributed to case selection bias. The first factor is that the date of the approval of rituximab for low-grade B-cell lymphoma preceded that for DLBCL for 2 years in Japan. The second factor is that FL were rebiopsied more frequently than DLBCL because FL relapsed frequently and were followed up for a long time, and checks for transformation to DLBCL were sometimes necessary.

Sixteen cases (27%) showed loss of CD20 expression in post-rituximab specimens by IHC or flow cytometry. The frequencies of CD20 loss in the various histological subtypes were: FL, 26% (9/34); DLBCL, 36% (4/11); MCL, 0% (0/10); MZBCL, 50% (1/2); and CLL, 100% (2/2). Among them, two DLBCL and two FL showed partial loss of CD20 expression. Among the 12 tumors with complete loss of CD20 expression, seven had available flow cytometry data, and all of them showed loss of CD20.

Four patterns of loss of CD20 expression were evident (Table 2): pattern 1, CD20 loss with no remarkable histological change (FL, 5; DLBCL, 3; and CLL, 2) (Fig. 1); pattern 2, proliferation of plasmacytoid cells (FL, 2; DLBCL, 1; and MZBCL, 1) (Fig. 2); pattern 3, transformation to classical Hodgkin lymphoma (FL, 1); and pattern 4, transformation to anaplastic large cell lymphoma (ALCL)-like undifferentiated lymphoma (FL, 1) (Fig. 3). All of the lymphomas after rituximab treatment with pattern 1 or 2 histology were positive for CD79a. Two FL with pattern 2 showed proliferation of plasmacytoid cells, not in the marginal zone but in follicles, as with FL with plasma cells,[27,28] and the plasmacytoid tumor cells were positive for IgM and Igκ by IHC. One DLBCL with pattern 2 was negative for IgM and Igλ by IHC in the pre-rituximab specimen, but positive for them in the post-rituximab specimen. Hodgkin lymphoma with pattern 3, which was previously reported to be a form of transformed FL,[29] was positive for CD30, CD15, and the IGH–BCL2 fusion by FISH, and negative for CD10, CD20, and EBER-1 by ISH. Although we could not determine the lineage of ALCL-like undifferentiated lymphoma with pattern 4, because it was positive for only CD45 and CD45RO and negative for CD3, CD5, CD7, CD10, CD15, CD20, CD30, CD56, CD79a, ALK, bcl-2, bcl-6, granzyme B, MPO, MUM1, PAX5, TdT, TIA-1, and EBER-1 by ISH, it was considered to be transformed FL because of the presence of the IGHBCL2 fusion revealed by FISH in both the pre- and post-rituximab specimens (Fig. 3).

Relationship between rituximab therapy and CD20 expression, and histological changes. The relationships between CD20 expression and interval after the last dose of rituximab, treatment regimens, clinical response, and frequency of rituximab administration were not detected. Among 16 cases showing loss of CD20, the clinical response to treatment was no change (NC) in three cases, and CR or partial response (PR) in the others.

Fourteen patients underwent rebiopsy within 1 month of the last dose of rituximab. Among them, only three cases (21%) were negative for CD20. Seven cases showing loss of CD20 expression after rituximab therapy were subsequently observed and rebiopsied and, among them, two cases (cases FL4-2 and FL8) regained CD20 expression at 7 and 15 months after the last dose of rituximab. The other five cases were found not to have regained CD20 expression at 2, 7, 12, 28, and 44 months after the last dose of rituximab.

Nine patients with FL achieved CR or PR after treatment with a rituximab-containing regimen, but their lymphomas showed early relapse (within 3 months to 1 year later). Among them, five cases (cases FL12, FL18, FL25, FL33, and FL34) relapsed as CD20-positive DLBCL, two (cases FL16 and FL21) as CD20-positive low-grade FL, one (case FL3-2) as CD20-negative FL grade 2, and one (case FL8) as transformation to Hodgkin's lymphoma.

Table 1. Patient characteristics

Case	Age (years)/sex	Stage	Pre-rituximab diagnosis (sample)	Therapy and response between biopsy and operation	Post-rituximab diagnosis (sample)	Post-rituximab interval (months)†	CD20 expression (%)	Histology by immunohistochemistry	Pattern
FL1	55/M	4	FL, gr.2 (LN)	Rx4, NC	FL, gr.1 (BM)	3	0	NHC	1
FL2	52/M	4	FL, gr.2 (LN)	C-MOPPx8, PR, Rx4, NC	FL, gr.1 (BM)	22	0	NHC	1
FL3-1	52/M	3	FL, gr.1 (LN)	R-CHOPx6, CR	FL, gr.2 (BM)	33	100	NHC	
FL3-2				Rx8+C-MOPPx5, CR, relapse, R-ICEx2, PR	FL, gr.2 (LN)	6	0	NHC	1
FL4-1	42/F	4	FL, gr.1 (LN)	Rx8+C-MOPPx16, NC	FL, gr.1 (BM)	23	100	NHC	
FL4-2				Rx8, NC	FL, gr.1 (BM)	5 days	0	NHC	1
FL5	59/M	4	FL, gr.2 (LN)	Rx4, NC, C-MOPPx13, PD, R-C-MOPPx8, CR	FL, gr.2 (BM)	21	–‡	NHC	1
FL6	40/M	4	FL, gr.1 (LN)	R-CHOPx6, CR	FL, gr.2 (LN)	12	90	Partially plasmacytoid cells (IgM+/Igκ+/CD138–)	2
FL7	49/F	4	FL, gr.1 (duodeunum)	R-CHOPx6, CR	FL, gr.1 (LN)	17	90	Partially plasmacytoid cells (IgM+/Igκ+/CD138–)	2
FL8	61/F	4	DLBCL+FL, gr.3a (LN)	Rx4+CHOPx8, CR	HL, MC (LN)	11	0	Transformation to HL	3
FL9	68/M	4	FL, gr.2 (LN)	R-C-MOPPx6, R-C-MOPPx8, relapse, fludarabine + Rx3	ALCL-like (liver)	18 days	0	Transformation to ALCL-like	4
L10	76/F	4	FL, gr.2 (LN)	Rx8, NC	FL, gr.2 (BM)	6	100	NHC	
FL11	54/F	4	FL, gr.2 (LN)	R-CHOPx6, CR	FL, gr.1 (BM)	15 days	100	NHC	
FL12	40/F	4	FL, gr.1 (LN)	CHOPx6, CR, relapse, C-MOPPx4, NC, Rx4, CR	DLBCL (colon)	4	100	Transformation to DLBCL	
FL13	44/M	4	FL, gr.2 (LN)	R-CHOPx6, PR, C-MOPPx6 radiation, PR	DLBCL+FL, gr.1 (BM)	59	100	Transformation to DLBCL	
FL14	47/M	4	FL, gr.2 (LN)	COPPx6, NC, Rx4, PD	FL, gr.1 (BM)	1	100	NHC	
FL15	43/M	4	FL, gr.1 (LN)	Rx4+C-MOPPx2, CR, zevalin, CR	FL, gr.1 (orbit)	26	100	NHC	
FL16	61/F	4	FL, gr.1 (BM), DLBCL (skin)	R-CHOPx8, CR	FL, gr.2 (LN)	9	100	NHC	
FL17	48/F	4	FL, gr.2 (LN)	Rx4+CHOPx6, PR	FL, gr.1 (BM)	23	100	NHC	
FL18	60/F	3	FL, gr.2 (LN)	Rx4, CR	DLBCL (tonsil)	4	100	Transformation to DLBCL	
FL19	54/F	4	FL, gr.1 (BM, stomach)	R-CHOPx6, PR	FL, gr.1 (BM)	37	100	NHC	
FL20	54/F	4	FL, gr.1 (LN)	Rx4, PR, CHOPx8, PR	FL, gr.2 (cecum)	36	100	NHC	
FL21	61/F	4	FL, gr.2 (LN)	R-CHOPx8, PR	FL, gr.1 (BM)	5	100	NHC	
FL22	66/F	3	FL, gr.2 (LN)	R-CHOPx8, PR	FL, gr.2 (skin)	26	100	NHC	
FL23	53/F	4	FL, gr.2 (ileum, colon)	R-CHOPx8, NC	FL, gr.1 (duodenum)	10	100	NHC	
FL24	51/F	4	FL, gr.2 (duodenum)	Rx1 (within R-CHOP)	FL, gr.1 (duodenum)	4 day	100	NHC	
FL25	55/M	3	DLBCL+FL, gr.3b (LN)	R-CHOPx8, CR	DLBCL (LN)	3	100	NHC	
FL26	37/M	4	FL, gr.2 (LN)	Rx2 (within R-CHOP)	FL, gr.2 (duodenum)	8 days	100	NHC	
FL27	62/M	4	FL, gr.1 (ileum)	Rx3 (within R-CHOP)	FL, gr.1 (duodenum)	8 days	100	NHC	
FL28	57/F	4	FL, gr.3a (LN)	Rx4, NC	DLBCL (LN)	3	100	Transformation to DLBCL	
FL29	51/M	3	DLBCL+FL, gr.3b (LN)	R-CHOPx6+Rx8, CR	DLBCL (LN)	21 days	100	NHC	
FL30	60/M	1	FL, gr.1 (duodenum)	Rx8, CR	FL, gr.1 (duodenum)	4 days	100	NHC	
FL31	63/M	1	FL, gr.1 (duodenum)	Rx8, PR	FL, gr.1 (duodenum)	1	100	NHC	
FL32	75/F	4	FL, gr.1 (BM)	Rx3	FL, gr.1 (BM)	4 days	100	NHC	
FL33	77/M	4	DLBCL+FL, gr.3a (pharynx)	R-CHOPx8, CR	DLBCL (LN)	8	100	NHC	

doi: 10.1111/j.1349-7006.2008.01005.x

Table 1. Continued

Case	Age (years)/sex	Stage	Pre-rituximab diagnosis (sample)	Therapy and response between biopsy and operation	Post-rituximab diagnosis (sample)	Post-rituximab interval (months)†	CD20 expression (%)	Histology by immunohistochemistry	Pattern
FL34	65/M	3	FL, gr.3a (LN)	Rx8, CR	DLBCL (LN)	5	100	Transformation to DLBCL	
DLBCL1-1	47/M	2	DLBCL (right testis)	R-CHOPx8, CR	DLBCL (left testis)	2	100	NHC	
DLBCL1-2				R-IVACx3, CR, BMT, CR	DLBCL (BM)	4	0	NHC	1
DLBCL2	71/M	3	DLBCL (ileum)	R-CHOPx8, CR, Rx1	DLBCL (LN)	10 days	10	NHC	1
DLBCL3	55/M	4	DLBCL (tonsil)	R-CHOPx8, PR	DLBCL (LN)	3	70	NHC	1
DLBCL4	58/F	2	DLBCL (EBER-1+) (stomach)	R-CHOPx8, PR	DLBCL (stomach)	4	0	Plasmacytoid cells (IgM+/Igλ+/CD138–)	2
DLBCL5	80/M	2	DLBCL (LN)	R-CHOPx8, CR	DLBCL (subcutaneous)	6	100	NHC	
DLBCL6	60/F	4	DLBCL (breast)	Chemotherapy, Rx4, CR	DLBCL (breast)	29 days	100	NHC	
DLBCL7	61/F	2	DLBCL (tonsil)	R-EPOCHx4, CR	DLBCL (colon, rectum)	16	100	NHC	
DLBCL8	75/F	4	DLBCL (stomach,duodenum)	R-CHOPx8, CR	DLBCL (stomach, duodenum)	30	100	NHC	
DLBCL9	65/F	3	DLBCL (LN)	Rx8+CHOPx6, PD	DLBCL (LN)	3	100	NHC	
DLBCL10	64/M	2	DLBCL (stomach)	Rx1+CHOPx2 (within R-CHOP)	DLBCL (stomach)	20 days	100	NHC	
DLBCL11	63/M	2	DLBCL (LN)	Rx8+CHOPx5+radiation, CR	DLBCL (LN)	8	100	NHC	
MCL1	72/M	4	MCL (LN)	R-CHOPx4, PR, Rx4, NC, COPx6, PD, R-CNOPx6, PD, cladribine, PD	MCL (stomach)	10 days	100	NHC	
MCL2	76/M	4	MCL (LN)	R-CHOPx8, PR	MCL (BM)	20	100	NHC	
MCL3	68/M	4	MCL (BM)	Rx1+CHOPx6, PR	MCL (BM)	1	100	NHC	
MCL4	66/M	4	MCL (colon)	R-CHOPx8, CR	MCL (stomach)	30	100	NHC	
MCL5	55/M	4	MCL (tonsil)	Rx4, PR	MCL (tongue)	28	100	NHC	
MCL6	59/F	4	MCL (stomach)	Rx4, PR, C-MOPPx8+ radiation+COP, PD	MCL (bone)	21	100	NHC	
MCL7-1	63/F	4	MCL (LN)	Rx4+C-MOPPx8, CR	MCL (stomach, duodenum)	17	100	NHC	
MCL7-2				Rx4, PR	MCL (stomach)	1	100	NHC	
MCL8	54/F	4	MCL (ileum)	Rx8+CHOPx6, CR	MCL (small intestine)	3	100	NHC	
MCL9	78/M	4	MCL (stomach)	Rx8, PD	MCL (orbit)	2	100	Change to blastoid variant	
MCL10	70/M	4	MCL (LN)	R-CHOPx8, PR	MCL (stomach)	18	100	NHC	
MZBCL1	68/F	3	MZBCL (LN)	R-ICEx1, CR	MZBCL (tonsil)	15	0	Plasmacytoid cells	2
MZBCL2	55/M	4	MZBCL (BM)	R-CHOPx6, PR	MZBCL (BM)	4	100	NHC	
CLL1	54/M	4	CLL (BM)	Rx2+C-MOPPx6, PR	CLL (LN)	12 days	0	NHC	1
CLL2	52/F	4	CLL (BM)	CHOPx8, COPx10, R-CEPPx7, R-ESHAPx2, CHASEx2, R-ESHAP+PBSCT, Rx5, PR	CLL (BM)	11	0	NHC	1

†From last dose of rituximab; ‡by flow cytometry. ALCL, anaplastic large cell lymphoma; BM, bone marrow; BMT, bone marrow transplantation; CEPP, cyclophosphamide, etoposide, procarbazine, and prednisolone; CHASE, cyclophosphamide, cytosine arabinoside, etoposide, and dexamethasone; CHOP, cyclophosphamide, doxorubicin, vincristine, and prednisone; CLL, chronic lymphocytic leukemia; C-MOPP, cyclophosphamide, vincristine, prednisone, and procarbazine; CR, complete response; diff., differentiation; DLBCL, diffuse large B-cell lymphoma; EPOCH, etoposide, prednisone, vincristine, cyclophosphamide, and doxorubicin; ESHAP, etoposide, methylprednisolone, high-dose cytarabine, and cisplatin; FL, follicular lymphoma; HL, Hodgkin's lymphoma; ICE, ifosfamide, carboplatin, and etoposide; IVAC, ifosfamide, vincristine, and cytarabine; LN, lymph node; MC, mixed cellularity; MCL, mantle cell lymphoma; MZBCL, marginal zone B-cell lymphoma; NC, no change; NHC, no remarkable histological change; PBSCT, peripheral blood stem cell transplantation; PD, progressive disease; PR, partial response; R, rituximab.

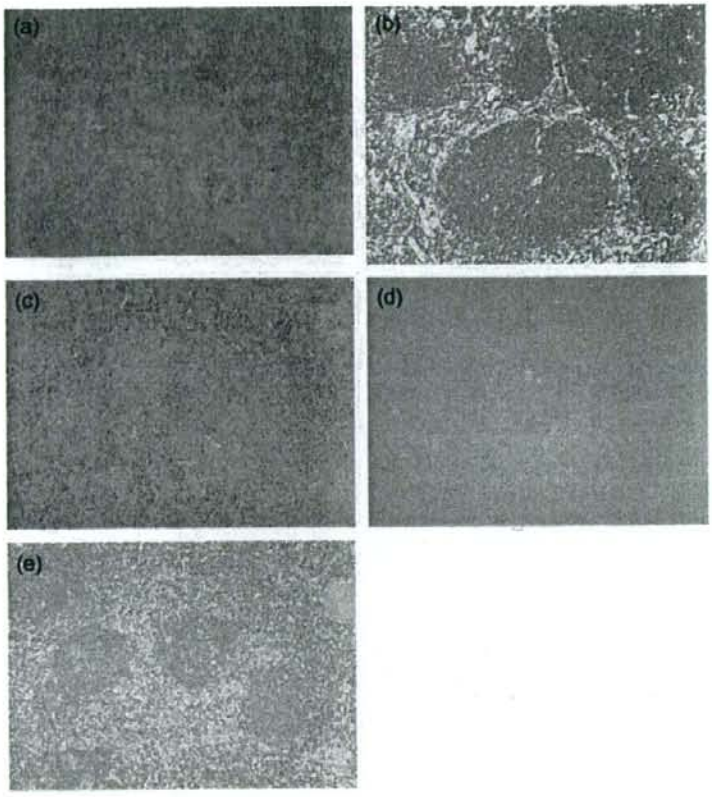

Fig. 1. (a–e) A case of pattern 1 change in CD20-positive follicular lymphoma (FL) to CD20-negative FL. FL, grade 1, (a) in a lymph node (hematoxylin–eosin, ×40) and (b) with CD20-positive phenotype, pre-rituximab (×100). FL, grade 2, (c) in a lymph node (hematoxylin–eosin, ×40) with (d) CD20-negative (×40) and (e) CD79a-positive (×40) phenotypes, post-rituximab.

Table 2. Four histological patterns of loss of CD20 expression after rituximab therapy

Histological pattern	Distribution
Pattern 1: loss of CD20 with no remarkable histological change	FL, 5; DLBCL, 3; CLL, 2
Pattern 2: proliferation of plasmacytoid cells	FL, 2; DLBCL, 1; MZBCL, 1
Pattern 3: transformation to classical Hodgkin lymphoma	FL, 1
Pattern 4: transformation to anaplastic large cell lymphoma-like undifferentiated lymphoma	FL, 1

CLL, chronic lymphocytic leukemia; DLBCL, diffuse large B-cell lymphoma; FL, follicular lymphoma; MZBCL, marginal zone B-cell lymphoma.

Discussion

Recent reports have indicated that the treatment of B-NHL with rituximab may be associated with CD20-negative lymphoma relapse,[5–17] and the frequency of loss of CD20 after rituximab treatment varies widely (24, 56, 60, and 94%).[9,11,13,14] In the present study, 16 of 59 B-NHL (27%) showed loss of CD20 after rituximab-containing therapy using a larger series than in previous reports. Our results also suggested that the frequency of CD20 loss was not largely affected by the period before rebiopsy. Although the site of sampling (bone marrow vs non-bone marrow) might affect the observed degree of CD20 loss,[9] this issue needs to be studied further using a larger number of cases. Tumors with loss of CD20 in the present study included FL, DLBCL, MZBCL, and CLL. Although Goteri *et al.* reported that MCL frequently showed loss of CD20 expression in bone marrow, none of our MCL cases showed CD20 loss.[13] Because a previous report indicated that rituximab + CHOP combination therapy (R-CHOP) had insufficient efficacy for MCL,[30] it was considered that this regimen might not have been sufficiently potent to induce selection of a CD20-negative clone.

Four histological patterns of CD20 loss were evident. The majority were patterns 1 or 2, whereas patterns 3 or 4 were rare. Recently, several reports have described relapse with pattern 1 or 2 histology after rituximab therapy.[13,16] Using flow cytometry, Goteri *et al.* demonstrated that 26 cases of low-grade B-cell lymphoma showed CD20 loss in bone marrow aspirates, including cases with no histological change, and with residual plasmacytoid tumor cells of lymphoplasmacytic lymphoma.[13] It has also been reported that mucosa-associated lymphoid tissue lymphoma changes to a pure plasma-cell neoplasm.[16]

Case FL8, which showed transformation to Hodgkin lymphoma (pattern 3), was one of the transformed FL that we reported previously.[29] As composite Hodgkin lymphoma and FL is reported to be very rare,[31,32] rituximab might have induced transformation to Hodgkin lymphoma. Recently, a case

doi: 10.1111/j.1349-7006.2008.01005.x

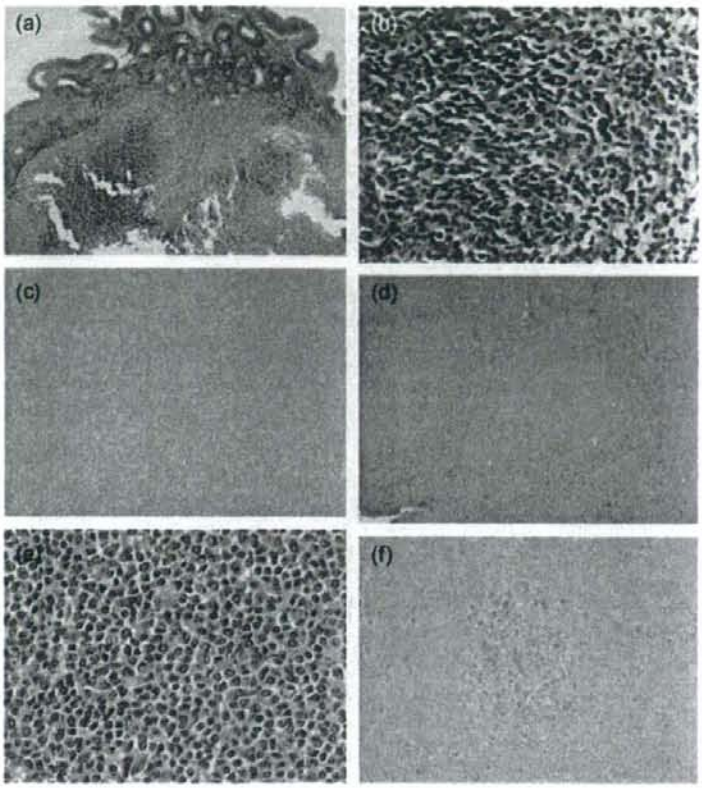

Fig. 2. (a–f) A case of pattern 2 change of follicular lymphoma (FL) to FL with plasma cells. FL, grade 1 in duodenum (hematoxylin–eosin), (a) ×40, (b) ×400, with (c) IgM-negative phenotype (×100), pre-rituximab. FL, grade 1 with plasmacytoid differentiation in lymph node (hematoxylin–eosin), (d) ×40, (e) ×400, with (f) IgM-positive phenotype (×100), post-rituximab.

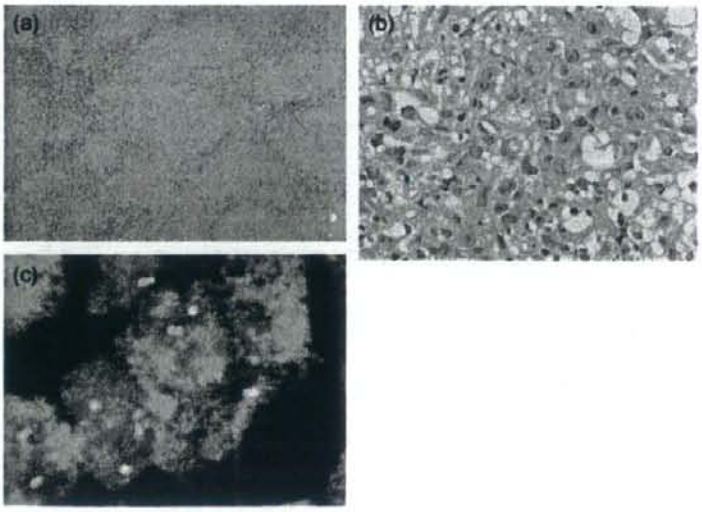

Fig. 3. (a–c) A case of pattern 4 change of follicular lymphoma (FL) to anaplastic large-cell lymphoma (ALCL)-like undifferentiated lymphoma. (a) FL, grade 2 in lymph node, pre-rituximab (hematoxylin–eosin, ×40). (b) ALCL-like undifferentiated lymphoma in liver, post-rituximab (hematoxylin–eosin, ×400). (c) The result of fluorescence *in situ* hybridization of ALCL-like undifferentiated lymphoma. IGH and BCL2 fusion pattern. Two fusion IGHBCL2 signals were present.

of Hodgkin lymphoma subsequent to FL in a patient receiving maintenance rituximab was reported.[17]

Transformation from FL to ALCL-like undifferentiated lymphoma (pattern 4) has been reported previously as neither transformation of FL nor histological change after rituximab therapy. Although two cases of FL with relapse to peripheral T-cell lymphoma after rituximab have been reported,[33,34] it was suspected that the T-cell lymphomas were another clone, thus differing from the present case. Cohen *et al.* reported large-cell transformation of CLL and FL during or soon after treatment with a fludarabine- and rituximab-containing regimen,[35] thus resembling the present case treated with fludarabine and rituximab.

Several mechanisms of resistance to rituximab have been suggested, including selection of a CD20-negative clone as a consequence of rituximab exposure, masking of CD20 epitopes by rituximab itself, or true loss of CD20 antigen due to genetic and epigenetic changes.[12,13,15,19–24] Although the present study was not intended to address the mechanism of CD20 loss, several remarkable phenomena were evident. No relationships were detected between loss of CD20 and the interval between the last dose of rituximab and rebiopsy, frequency of rituximab administration, clinical responses, and treatment regimens. It is suspected that susceptibility to rituximab differs greatly among lymphomas. Our results also indicated that loss of CD20 immediately after rituximab therapy was not frequent. Although some cases do regain CD20 expression, loss of CD20 persisting for more than 6 months is not infrequent.

A previous case report has emphasized that early relapse of FL after rituximab therapy was related to CD20-negative transformation to DLBCL.[15] However, this was not confirmed in our study using a larger series: most of the relapses were CD20-positive DLBCL, and only two were CD20-negative FL or Hodgkin lymphoma. Our results suggested that CD20-positive relapse with histological transformation occurred most frequently in cases of early relapse, and that CD20-negative relapse was relatively rare.

In conclusion, our findings indicate that 27% of B-NHL show loss of CD20 expression with four histological patterns after rituximab therapy. As the changes in morphology and CD20 expression after rituximab therapy vary widely, including not only loss of CD20 expression but also proliferation of plasmacytoid cells or transformation to special subtypes of lymphoma, and clinical outcomes are very confused, careful follow up and rebiopsy are recommended.

Acknowledgments

The authors are grateful to Ms S. Miura and Ms C. Kina for their excellent technical assistance.

References

1 Reff ME, Carner K, Chambers KS *et al.* Depletion of B cells *in vivo* by a chimeric mouse human monoclonal antibody to CD20. *Blood* 1994; **83**: 435–45.
2 Demidem A, Lam T, Alas S *et al.* Chimeric anti-CD20 (IDEC-C2B8) monoclonal antibody sensitizes a B cell lymphoma cell line to cell killing by cytotoxic drugs. *Cancer Biother Radiopharm* 1997; **12**: 177–86.
3 Shan D, Ledbetter JA, Press OW. Apoptosis of malignant human B cells by ligation of CD20 with monoclonal antibodies. *Blood* 1998; **91**: 1644–52.
4 Cardarelli PM, Quinn M, Buckman D *et al.* Binding to CD20 by anti-B1 antibody or F(ab')(2) is sufficient for induction of apoptosis in B-cell lines. *Cancer Immunol Immunother* 2002; **51**: 15–24.
5 Meeker T, Lewder J, Cteary ML *et al.* Emergence of idiotype variants during treatment of B-cell lymphoma with anti-idiotype antibodies. *N Eng J Med* 1985; **312**: 1658–65.
6 Kinoshita T, Nagai H, Murate T *et al.* CD20-negative relapse in B-cell lymphoma after treatment with rituximab. *J Clin Oncol* 1998; **16**: 3916.
7 Davis TA, Czerwinski DK, Levy R. Therapy of B-cell lymphoma with anti-CD20 antibodies can result in the loss of CD20 antigen expression. *Clin Cancer Res* 1999; **5**: 611–15.
8 Schmitz K, Brugger W, Weiss B *et al.* Clonal selection of CD20-negative non-Hodgkin's lymphoma cells after treatment with anti-CD20 antibody rituximab. *Br J Haematol* 1999; **106**: 571–2.
9 Foran JM, Norton AJ, Micallef IN *et al.* Loss of CD20 expression following treatment with rituximab (chimaeric monoclonal anti-CD20): a retrospective cohort analysis. *Br J Haematol* 2001; **114**: 881–3.
10 Chu PG, Chen YY, Molina A *et al.* Recurrent B-cell neoplasms after Rituximab therapy: an immunophenotypic and genotypic study. *Leuk Lymphoma* 2002; **43**: 2335–41.
11 Kennedy GA, Tey SK, Cobcroft R *et al.* Incidence and nature of CD20-negative relapses following rituximab therapy in aggressive B-cell non-Hodgkin's lymphoma: a retrospective review. *Br J Haematol* 2002; **119**: 412–16.
12 Jilani I, O'Brien S, Manshuri T *et al.* Transient down-modulation of CD20 by rituximab in patients with chronic lymphocytic leukemia. *Blood* 2003; **102**: 3514–20.
13 Goteri G, Olivieri A, Ranaldi M *et al.* Bone marrow histopathological and molecular changes of small B-cell lymphomas after rituximab therapy: comparison with clinical response and patients' outcome. *Int J Immunopathol Pharmacol* 2006; **19**: 421–31.
14 Seliem RM, Freeman JK, Steingart RH *et al.* Immunophenotypic changes and clinical outcome in B-cell lymphomas treated with rituximab. *Appl Immunohistochem Mol Morphol* 2006; **14**: 18–23.
15 Alovaro-Naranjo TA, Jaen-Martinez JJ, Guma-Padro JG *et al.* CD20-negative DLBCL transformation after rituximab treatment in follicular lymphoma: a new case report and review of the literature. *Ann Hematol* 2003; **82**: 585–8.
16 Woehrer S, Streubel B, Chott A *et al.* Transformation of MALT lymphoma to pure plasma cell histology following treatment with the anti-CD20 antibody rituximab. *Leuk Lymphoma* 2005; **46**: 1645–9.
17 Scaramucci L, Perrotti A, Niscola P *et al.* Hodgkin disease subsequent to follicular lymphoma on maintenance rituximab. *Leuk Lymphoma* 2007; **48**: 1878–80.
18 Pijuan L, Vicioso L, Bellosillo B *et al.* CD20-negative T-cell-rich B-cell lymphoma as a progression of a nodular lymphocyte-predominant Hodgkin's lymphoma treated with rituximab: a molecular analysis using laser capture microdissection. *Am J Surg Pathol* 2005; **29**: 1399–403.
19 Cragg MS, Bayne MC, Illidge TM *et al.* Apparent modulation of CD20 by rituximab: an alternative explanation. *Blood* 2004; **103**: 3989–90.
20 Rawal YB, Nuovo GJ, Frambach GE *et al.* The absence of CD20 messenger RNA in recurrent cutaneous B-cell lymphoma following rituximab therapy. *J Cutan Pathol* 2005; **32**: 616–21.
21 Takei K, Yamazaki T, Sawada U *et al.* Analysis of changes in CD20, CD55, and CD59 expression on established rituximab-resistant B-lymphoma cell lines. *Leuk Res* 2006; **30**: 625–31.
22 Tomita A, Hiraga J, Kiyoi H *et al.* Epigenetic regulation of CD20 protein expression in a novel B-cell lymphoma cell line, RRBL1, established from a patient treated repeatedly with rituximab-containing chemotherapy. *Int J Hematol* 2007; **86**: 49–57.
23 Jazirehi AR, Vega MI, Bonavida B. Development of rituximab-resistant lymphoma clones with altered cell signaling and cross-resistance to chemotherapy. *Cancer Res* 2007; **67**: 1270–81.
24 Czuczman MS, Olejniczak S, Gowda A *et al.* Acquirement of rituximab resistance in lymphoma cell lines is associated with both global CD20 gene and protein down-regulation regulated at the pretranscriptional and posttranscriptional levels. *Clin Cancer Res* 2008; **14**: 1561–70.
25 Jaffe ES, Harris NL, Stein H *et al. World Health Organization Classification of Tumours Pathology & Genetics: Tumours of Haematopoietic and Lymphoid Tissues*. Lyon: IARC Press, 2001.
26 Sekiguchi N, Kobayashi Y, Yokota Y *et al.* Follicular lymphoma subgrouping by fluorescence *in situ* hybridization analysis. *Cancer Sci* 2005; **96**: 77–82.
27 Keith TA, Cousar JB, Glick AD *et al.* Plasmacytic differentiation in follicular center cell (FCC) lymphomas. *Am J Clin Pathol* 1985; **84**: 283–90.
28 Vago JF, Hurtubise PE, Redden-Borowski MM *et al.* Follicular center-cell lymphoma with plasmacytic differentiation, monoclonal paraprotein, and peripheral blood involvement: recapitulation of normal B-cell development. *Am J Surg Pathol* 1985; **9**: 764–70.
29 Maeshima AM, Omatsu M, Nomoto J *et al.* Diffuse large B-cell lymphoma after transformation from low-grade follicular lymphoma: morphological, immunohistochemical and FISH analyses. *Cancer Sci* 2008; **99**: 1760–8.
30 Lenz G, Dreyling M, Hoster E *et al.* Immunochemotherapy with rituximab and cyclophosphamide, doxorubicin, vincristine, and prednisone significantly improves response and time to treatment failure, but not long-term outcome in patients with previously untreated mantle cell lymphoma: results of a

doi: 10.1111/j.1349-7006.2008.01005.x

prospective randomized trial of the German Low Grade Lymphoma Study Group (GLSG). *J Clin Oncol* 2005; **23**: 1984–92.
31 Brauninger A, Hansmann ML, Strickler JG *et al.* Identification of common germinal-center B-cell precursors in two patients with both Hodgkin's disease and non-Hodgkin's lymphoma. *N Eng J Med* 1999; **340**: 1239–47.
32 Marafioti T, Hummel M, Anagnostopoulos I *et al.* Classical Hodgkin's disease and follicular lymphoma originating from the same germinal center B cell. *J Clin Oncol* 1999; **17**: 3804–9.
33 Micallef IN, Kirk A, Norton A *et al.* Peripheral T-cell lymphoma following rituximab therapy for B-cell lymphoma. *Blood* 1999; **93**: 2427–8.
34 Tetreault S, Abler SL, Robbins B *et al.* Peripheral T-cell lymphoma after anti-CD20 antibody therapy. *J Clin Oncol* 1998; **16**: 1635–7.
35 Cohen Y, Da'as N, Libstet D *et al.* Large-cell transformation of chronic lymphocytic leukemia and follicular lymphoma during or soon after treatment with fludarabine-rituximab-containing regimens: natural history- or therapy-related complication? *Eur J Haematol* 2002; **68**: 80–3.

JOURNAL OF BIOSCIENCE AND BIOENGINEERING
Vol. 105, No. 1, 81–84. 2008
DOI: 10.1263/jbb.105.81

Proposal of New Gene Filtering Method, BagPART, for Gene Expression Analysis with Small Sample

Takashi Kawamura,[1] Hiro Takahashi,[1§] and Hiroyuki Honda[1,2]*

Department of Biotechnology, School of Engineering, Nagoya University, Furo-cho, Chikusa-ku, Nagoya 464-8603, Japan[1] and MEXT Innovative Research Center for Preventive Medical Engineering, Nagoya University, Furo-cho, Chikusa-ku, Nagoya 464-8603, Japan[2]

Received 25 July 2007/Accepted 8 October 2007

A significant problem in gene expression analysis is that the sample size is substantially lower than the number of genes. Bagging is an effective method of solving this problem in the case of small sample datasets. We have devised a combination method, called the BagPART filtering method, that uses the projective adaptive resonance theory (PART) to select important genes and achieve a binary classification more accurately ($p<10^{-10}$) than conventional methods, particularly when the sample size is small.

[**Key words:** gene expression analysis, bootstrap aggregating, projective adaptive resonance theory, gene filtering method, boosted fuzzy classifier with SWEEP]

In gene expression analysis, filtering methods are needed to avoid the problem of dimensions. A number of methods have been developed to solve this problem; these include signal-to-noise (S2N) measurement, significance analysis of microarrays (SAM), and nearest shrunken centroid (NSC) (1–3). We developed a projective adaptive resonance theory (PART) filtering method for gene expression analysis by modifying the original PART filtering method reported in our previous studies (4, 5). Currently, we can obtain gene expression information from more than 10,000 genes owing to advanced DNA microarray technology; however, the sample size is, at most, about 100 in most datasets. Thus, the sample size is much smaller than the number of genes. We have improved the PART filtering method by introducing the idea of bootstrap aggregating (Bagging) (6). We have designated the new method as BagPART. We applied BagPART to the analysis of the two gene expression profile datasets and compared its results with those of PART. In addition, we tested the performance of both methods in the case of a small sample size. As a result, we have shown that BagPART is statistically superior to PART for each dataset, and that BagPART is more effective when sample size is small.

We used two sets of gene expression profiles downloaded from the Stanford Microarray Database (http://genome-www5.stanford.edu). The first set consisted of the colon cancer gene expression profiles reported by Alon *et al.* (7). This dataset comprised 2000 genes and 62 samples (40 tumor samples and 22 normal samples). The second set consisted of the prostate cancer gene expression profiles reported by Singh *et al.* (8). This dataset comprised 12,600 genes and 102 samples (52 tumor samples and 50 normal samples). We selected only those genes for which all the 102 samples showed a positive intensity, resulting in the selection of 1820 genes. Signal values were transformed to a common logarithm. For the colon dataset, because the tumor sample number is about twice as large as that of normal controls, we randomly selected tumor samples to equal the number of normal samples.

BagPART modifies the PART algorithm in the following manner. Assume that we have an original dataset $S=\{(x_1, y_1), ..., (x_n, y_n)\}$ of size n, where x_i represents the feature and y_i is the class label of the observation (x_i, y_i). We draw bootstrap datasets with the replacement $S_b^*=\{(x_1^*, y_1^*), ..., (x_n^*, y_n^*)\}$, $b=1, ..., B$ for a large B (between 50 and 200). In the bootstrap dataset, a sample is randomly selected and some degree of overlap within the sample is permitted. For each bootstrap dataset S_b^*, we carry out PART and extract the gene group G_b. We repeat this procedure for all bootstrap datasets, $S_1^*, ..., S_B^*$, and finally select genes that are included in more than half of the B gene groups, $G_1, ..., G_B$. A schematic diagram of this process is shown in Fig. 1.

A parallel comparison of PART and BagPART was carried out. Firstly, all the samples were randomly divided into two groups: one was designated a training group, which helped to construct classification models, and the other was designated a test group, which was used to evaluate the model constructed by the training group. The distributions of normal and tumor samples were equal for both groups. To investigate the performance of each model in the cases where the number of samples in the training group was small, the training sample size was changed to three patterns. The ratios of the training sample size to the total number of samples, hereafter expressed as training sample ratio (TSR), were 0.8, 0.6, and 0.4. Table 1 shows the number of samples used in the analysis of each expression dataset. Secondly, to se-

* Corresponding author. e-mail: honda@nubio.nagoya-u.ac.jp
phone: +81-(0)52-789-3215 fax: +81-(0)52-789-3214
§ Present address: College of Bioscience and Biotechnology, Chubu University, 1200 Matsumoto-cho, Kasugai, Aichi 487-8501, Japan.

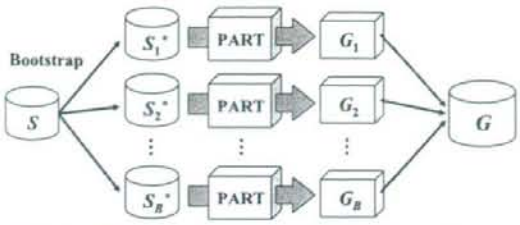

FIG. 1. Schematic image of BagPART. In the first step, the resampling data S_1^*, S_2^*, ..., S_B^* are made using bootstrap from the original data S. In the second step, the genes sets G_1, G_2, ..., G_B are extracted by PART from each resampling dataset. Finally, genes included in more than half of the B gene sets are selected. The selected gene set is represented as G.

lect genes used to construct classification models, BagPART and the PART filtering method were each applied to the training group, and about 100 genes were returned by each method in both expression datasets. In the BagPART algorithm, we used $B=100$, which was adequate to converge the selected gene size (Fig. 2). Finally, classification models were constructed from the training group using only information on extracted genes and the estimated test group. Here, we used the Boosted Fuzzy Classifier with SWEEP operator method (BFCS), we developed in a previous study, which constructs 10 models for various gene combinations (9). We repeated these operations 10 times, and tested whether there is a statistically significant difference between the results using a paired t-test.

TABLE 1. Number of samples in each dataset

TSR*	Training sample	Test sample
Dataset: Colon cancer (normal: 22, tumor: 22)		
0.8	36	8
0.6	26	18
0.4	18	26
Dataset: Prostate cancer (normal: 50, tumor: 52)		
0.8	82	20
0.6	61	41
0.4	41	61

* TSR, Training sample ratio, indicates the ratio of the number of training samples to the total number of samples.

Tables 2 and 3 show the results of our analysis of the colon cancer and prostate cancer gene sets, respectively. Both results showed that BagPART was statistically superior to

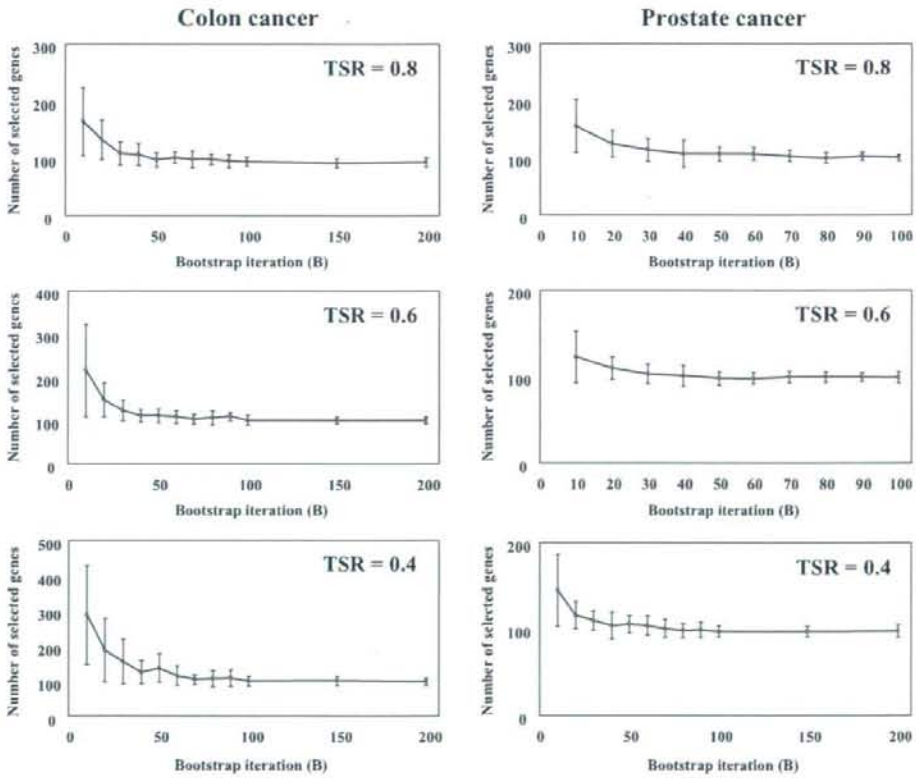

FIG. 2. Number of selected genes for each bootstrap iteration. BagPART was applied to each dataset 100 times and showed the average number of selected genes and standard deviation for each bootstrap iterations (B) in Fig. 1. The number of selected genes converged, and the standard deviation was very small in each dataset when B=100.

TABLE 2. Classification results of BagPART and PART for colon cancer dataset

TSR	Method	Average test accuracy (%)					Selected gene
		1 input	2 inputs	3 inputs	4 inputs	5 inputs	
0.8	BagPART	66.3[a]±6.6[b]	73.3±8.7	75.5±6.9	71.8±8.3	71.3±10.6	100[d]
	PART	60.3±7.2	61.0±8.3	68.1±10.0	69.0±8.3	70.9±11.2	99
	p-value			4.19×10^{-10}[c]			
0.6	BagPART	65.3±5.9	75.3±8.1	73.5±8.3	76.0±8.2	74.3±9.3	100
	PART	60.3±3.7	69.4±10.3	71.1±8.7	72.4±8.2	69.7±9.0	99
	p-value			5.30×10^{-11}			
0.4	BagPART	65.4±1.8	72.2±6.8	73.8±6.3	74.8±6.2	76.2±6.1	100
	PART	62.7±2.9	68.2±8.8	70.1±6.5	68.9±8.2	71.2±6.8	99
	p-value			2.16×10^{-14}			

[a] Average of test accuracies in 10 various datasets × 10 models.
[b] Standard deviation of test accuracies in 10 various datasets × 10 models.
[c] Result of paired t-test for comparison of test accuracies of BagPART with PART.
[d] The number of selected genes obtained from BagPART or PART. In BagPART, this is represented as *G* in Fig. 1.

TABLE 3. Classification results of BagPART and PART for prostate cancer dataset

TSR	Method	Average test accuracy (%)						Selected gene
		1 input	2 inputs	3 inputs	4 inputs	5 inputs	6 inputs	
0.8	BagPART	73.4±7.9	79.1±6.5	81.2±7.9	81.7±6.7	83.0±6.8	83.0±6.8	100
	PART	68.7±5.6	79.4±5.7	78.9±8.3	80.6±7.1	80.9±7.4	80.9±7.4	100
	p-value			1.70×10^{-5}				
0.6	BagPART	76.7±4.3	80.2±3.9	82.7±3.5	83.7±3.3	84.5±3.2	85.4±3.4	101
	PART	73.2±4.5	81.4±4.2	82.6±3.6	84.2±4.2	84.2±4.2	84.8±3.2	100
	p-value			4.58×10^{-2}				
0.4	BagPART	77.1±1.5	81.0±2.8	83.6±2.0	83.5±2.7	84.9±2.2	85.3±2.5	99
	PART	71.6±4.3	80.6±3.9	80.9±2.9	81.8±3.2	82.0±3.6	83.1±3.4	101
	p-value			2.48×10^{-13}				

PART. For the colon cancer dataset, it was clear that despite the smaller sample sizes in the training data, we observed smaller p values using BagPART than using PART. Thus, BagPART can correctly extract genes even if the sample size is small. For the prostate cancer dataset, when TSR decreased from 0.8 to 0.6, p increased p=from 1.70×10^{-5} to 4.58×10^{-2}. However, when TSR decreased to 0.4, p decreased markedly to 2.48×10^{-13}. This means that when TSR was between 0.8 and 0.6, the number of training samples in each dataset (82 samples and 61 samples, respectively), was sufficient to correctly extract genes with PART. In practice, we obtained a more significant value, $p=5.45\times10^{-15}$, when TSR decreased to 0.2 and the training sample size was 20 (data not shown). These results were in accord with previous results of Fu *et al.* (10). When the sample size is small, the performance of estimation models varies markedly depending on the proposal method. Many researchers have also reported that analytical methods using bootstrap could potentially provide more accurate estimates from datasets with small sample size.

We concluded that our method benefited from the bootstrap method. However, it is likely that when the sample size is too small, the performance of BagPART becomes poor. It is difficult to describe the minimum sample size needed for satisfactory results because the minimum sample size strongly depends on the quality of the dataset or complexity of the acquired model.

A number of genes appeared frequently in the outputs of the BagPART analysis of both datasets (Table 4). For the colon cancer dataset, in particular, the two genes, *MYH* and *COL11A2*, were frequently selected. *COL11A2* is one of two genes that encode two alpha strands of type11 collagen. *COL11A1* has been reported to be not expressed in a normal colon but to be upregulated in colorectal cancer (11). This gene was selected frequently in BagPART analysis when the TSRs were 0.8, 0.6, and 0.4. However, in regular PART analysis, this gene was only selected when TSR was 0.4, and was only the 11th most frequent gene to appear in the output (data not shown). *MYH* is relevant to DNA repair; *MYH* mutation causes familial adenomatous polyposis (FAP) (12, 13). This gene was also constantly selected in BagPART analysis regardless of TSR; however, in PART, it was not selected at all when TSR was 0.8.

MYH and *COL11A2* have been reported as important genes by many researchers, such as Le *et al.* (14), Shevade and Keerthi (15), Chu *et al.* (16), and Ma and Huang (17). However, when we employed PART as a filtering method, both genes were not frequently selected amongst all datasets. Thus, there is a substantial difference in results between PART and BagPART. For the prostate cancer dataset, *HPN* was frequently selected by both filtering methods. This gene has been reported as a marker of prostate cancer (20). Moreover, other genes, such as *AKR1B1* and *HSPD1*, which have been reported to play a role in prostate cancer (21), were frequently selected by BagPART, but not by PART (data not shown). These results indicate that BagPART can select meaningful genes even if the sample size is small. Moreover, BagPART could constantly select important genes in spite of the poor TSR values; we speculate that this characteristic is a result of using the bootstrap method.

TABLE 4. Gene lists selected frequently by BagPART

Rank	Gene ID	Genbank	Gene name	Description	Reference
Colon cancer					
1	Hsa.37937	R87126	MYH	Myosin heavy chain, nonmuscle (*Gallus gallus*)	16, 17
2	Hsa.6814	H08393	COL11A2	Collagen alpha 2(XI) chain (*Homo sapiens*)	16, 17
3	Hsa.549	R36977	GTF3A	general transcription factor III A	18, 19
4	Hsa.627	M26383	IL8	MONAP mRNA, complete cds.	17, 18
5	Hsa.21562	R08021	PPA1	Inorganic pyrophosphatase (*Bos taurus*)	–
Prostate cancer					
1	37639_at	X07732	HPN	Hepsin (transmembrane protease, serine 1)	19, 22
2	38406_f_at	AI207842	–	Homo sapiens cDNA, 3 end	17, 19
3	36589_at	X15414	AKR1B1	Aldo-keto reductase family 1, member B1 (aldose reductase)	19
4	40282_s_at	M84526	DF	D component of complement (adipsin)	19, 22
5	37720_at	M22382	HSPD1	Heat shock 60kDa protein 1 (chaperonin)	19, 23

We have developed an improved PART filtering method that uses Bagging. To investigate the effect of the new method, BagPART, on the gene expression analysis, we applied BagPART to two types of dataset, and obtained a significant difference between the two datasets. In addition, we have clarified that the new method could more correctly extract genes than conventional methods when the sample size is small. In this study, we compared BagPART with only PART. In our previous paper, we have reported that PART is superior to signal-to-noise (S2N) measurement and nearest shrunken centroid (NSC) (4). Therefore, we believe that BagPART has better performance than the other methods, although further comparison with other methods such as SOM has not yet been carried out. We believe that, in the case of precious or rare samples, our method is advantageous for extracting important genes.

REFERENCES

1. **Golub, T. R., Slonim, D. K., Tamayo, P., Huard, C., Gaasenbeek, M., Mesirov, J. P., Coller, H., Loh, M. L., Downing, J. R., Caligiuri, M. A., Bloomfield, C. D., and Lander, E. S.:** Molecular classification of cancer: class discovery and class prediction by gene expression monitoring. Science, **286**, 531–537 (1999).
2. **Tusher, V. G., Tibshirani, R., and Chu, G.:** Significance analysis of microarrays applied to the ionizing radiation response. Proc. Natl. Acad. Sci. USA, **98**, 5116–5121 (2001).
3. **Tibshirani, R., Hastie, T., Narasimhan, B., and Chu, G.:** Diagnosis of multiple cancer types by shrunken centroids of gene expression. Proc. Natl. Acad. Sci. USA, **99**, 6567–6572 (2002).
4. **Takahashi, H., Kobayashi, T., and Honda, H.:** Construction of robust prognostic predictors by using projective adaptive resonance theory as a gene filtering method. Bioinformatics, **21**, 179–186 (2005).
5. **Cao, Y. and Wu, J.:** Projective ART for clustering data sets in high dimensional spaces. Neural Netw., **15**, 105–120 (2002).
6. **Breiman, L.:** Bagging predictors. Mach. Learn., **24**, 123–140 (1996).
7. **Alon, U., Barkai, N., Notterman, D. A., Gish, K., Ybarra, S., Mack, D., and Levine, A. J.:** Broad patterns of gene expression revealed by clustering analysis of tumor and normal colon tissues probed by oligonucleotide arrays. Proc. Natl. Acad. Sci. USA, **96**, 6745–6750 (1999).
8. **Singh, D., Febbo, P., Ross, K., Jackson, D., Manola, J., Ladd, C., Tamayo, P., Renshaw, A., D'Amico, A., Richie, J., and other 5 authors:** Gene expression correlates of clinical prostate cancer behavior. Cancer Cell, **1**, 203–209 (2002).
9. **Takahashi, H. and Honda, H.:** A new reliable cancer diagnosis method using boosted fuzzy classifier with SWEEP operator method. J. Chem. Eng. Jpn., **38**, 763–777 (2005).
10. **Fu, W. J., Carroll, R. J., and Wang, S.:** Estimating misclassification error with small samples via bootstrap cross-validation. Bioinformatics, **21**, 1979–1986 (2005).
11. **Fisher, H., Stenling, R., Rubio, C., and Lindblom, A.:** Colorectal carcinogenesis is associated with stromal expression of COL11A1 and COL5A2. Carcinogenesis, **22**, 875–878 (2001).
12. **Varesco, L.:** Familial adenomatous polyposis: genetics and epidemiology. Tech. Coloproctol., **8**, 305–308 (2004).
13. **Ponti, G., Ponz de Leon, M., Maffei, S., Pedroni, M., Losi, L., Di Gregorio, C., Gismondi, V., Scarselli, A., Benatti, P., Roncari, B., and 6 authors:** Attenuated familial adenomatous polyposis and Muir-Torre syndrome linked to compound biallelic constitutional MYH gene mutations. Clin. Genet., **68**, 442–447 (2005).
14. **Li, Y., Campbell, C., and Tipping, M.:** Bayesian automatic relevance determination algorithms for classifying gene expression data. Bioinformatics, **18**, 1332–1339 (2002).
15. **Shavade, S. K. and Keerthi, S. S.:** A simple and efficient algorithm for gene selection using sparse logistic regression. Bioinformatics, **19**, 2246–2253 (2003).
16. **Chu, W., Ghahramani, Z., Falciani, F., and Wild, D. L.:** Biomarker discovery in microarray gene expression data with Gaussian processes. Bioinformatics, **21**, 3385–3393 (2005).
17. **Ma, S. and Huang, J.:** Regularized ROC method for disease classification and biomarker selection with microarray data. Bioinformatics, **21**, 4356–4362 (2005).
18. **Chen, J. J., Tsai, C., Tzeng, S., and Chen, C.:** Gene selection with multiple ordering criteria. BMC Bioinformatics, **8**, 74–90 (2007).
19. **Yap, Y., Zhang, X., Ling, M., Wang, X., Wong, Y., and Danchin, A.:** Classification between normal and tumor tissues based on the pair-wise gene expression ratio. BMC Cancer, **4**, 72–88 (2004).
20. **Xu, L., Tan, A. C., Naiman, D. Q., Geman, D., and Winslow, R. L.:** Robust prostate cancer marker genes emerge from direct integration of inter-study microarray data. Bioinformatics, **21**, 3905–3911 (2005).
21. **Johansson, B., Pourian, M. R., Chuan, Y. C., Byman, I., Berqh, A., Panq, S. T., Norstedt, G., Berqman, T., and Pousette, A.:** Proteomic comparison of prostate cancer cell lines LNCaP-FGC and LNCaP-r reveals heatshock protein 60 as a marker for prostate malignancy. Prostate, **66**, 1235–1244 (2006).
22. **Niijima, S. and Kuhara, S.:** Recursive gene selection based on maximum margin criterion: a comparison with SVM-RFE. BMC Bioinformatics, **7**, 543–560 (2006).
23. **Lai, Y., Wu, B., Chen, L., and Zhao, H.:** A statistical method for identifying differential gene-gene co-expression patterns. Bioinformatics, **20**, 3146–3155 (2004).